Molecular Dynamics Simulations of Mechanical Properties of Boron-Nitride Nanotubes Embedded in Si-B-N Ceramics

Michael Griebel and Jan Hamaekers

Department of Numerical Simulation, University of Bonn,
Wegelerstraße 6, D-53115 Bonn, Germany.
e-mail: griebel@ins.uni-bonn.de, hamaekers@ins.uni-bonn.de

ABSTRACT

The elastic properties of BN-nanotubes embedded in amorphous Si-B-N matrices are examined by classical molecular dynamics simulations (MD) using the Parrinello-Rahman approach. To this end, all systems are modeled with a reactive many-body bond order potential due to Tersoff. We apply external stress and derive stress-strain curves for various tensile load cases at given temperature and pressure. In addition to Young moduli and Possion ratios, we compare radial distribution functions, average coordination numbers, ring statistics and self-diffusion coefficients in order to characterize the short-range, medium-range and long-range order of Si_3BN_5, $Si_3B_2N_6$ and $Si_3B_3N_7$ matrices. Here, our results show that $Si_3B_3N_7$ exhibits the highest Young modulus and the largest elastic range. Furthermore, we calculate stress-strain curves for BN-NTs embedded in Si-B-N matrices to predict the rates of reinforcement of the ceramics composites. Here the influence of the NT/matrix ratio on the elastic modulus is examined and we compare the derived Young moduli with predictions related to macroscopic rule-of-mixtures.

1 Introduction

Boron nitride nanotubes (BN-NTs) share many of the exceptional properties of carbon nanotubes (C-NTs). In particular, experimental studies and numerical simulations of their mechanical properties show that BN-NTs display a high Young modulus which is comparable to that of C-NTs. In contrast to C-NTs, BN-NTs exhibit an energy gap of about 4-5 eV independent of chirality, diameter and number of walls. Altogether, BN-NTs are one of the strongest insulating nanofibers and may find important uses in the reinforcement of amorphous materials. On the other hand, amorphous Si-N based systems containing B exhibit a diversity of industrial applications because of their unusual thermal and mechanical properties. Therefore, it can be expected that BN-NTs embedded in a Si-B-N matrix result in a promising future material. Note that, to our knowledge, composites of Si-B-N ceramics and BN-NTs have neither been theoretically studied nor been synthesized so far. Here, computational methods can be used to access and thus to predict, to describe and to explain characteristic properties of such future materials [1]. For large systems with thousand atoms and more, classical MD simulations are an important tool to better understand mechanical

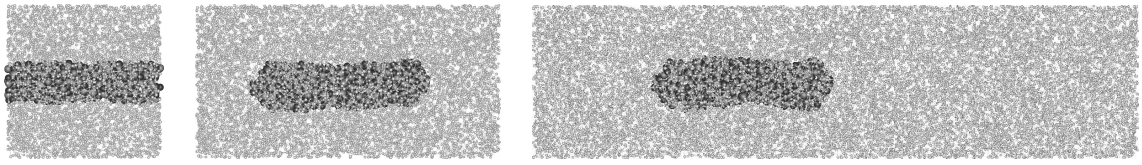

II III IV

Figure 1: Equilibrated System II, System III and System IV.

and thermal properties of BN-NT Si-B-N ceramics composites. In this work, we analyze the short-range, medium-range and long-range order and the mechanical and thermal properties of amorphous Si_3BN_5, $Si_3B_2N_6$ and $Si_3B_3N_7$ matrices by molecular dynamics simulations. Our results show that amorphous $Si_3B_3N_7$ exhibits the highest Young modulus and the largest elastic range. Therefore we concentrate on BN-NT $Si_3B_3N_7$ ceramics composites. Here, we derive stress-strain curves at various temperatures for different NT/matrix ratios. Finally, we compare our results with two macroscopic rule-of-mixtures, which are commonly used to predict the Young modulus and thus to derive the rate of reinforcement of composites.

2 Computational Methods

In our MD simulations, we use a reactive many-body bond-order potential model due to Tersoff, which is able to accurately describe covalent bonding. Because all interatomic terms are of short range, we use the well-known linked cell technique [1]. A straightforward domain decomposition approach then allows for a parallel implementation, which results in a parallel complexity of the order $\mathcal{O}(N/P)$ [2, 1]. Here, N denotes the number of particles and P the number of processors. To deal with the equilibration of the systems at given temperature and pressure, we apply a so-called Parrinello-Rahman-Nosé Lagrangian. Based on this method, we use an additional external stress-tensor to account for various tensile load cases [3, 4]. In particular, we increase or decrease linearly the uniaxial external stress components over time to generate stress-strain curves. Then, assuming a linear stress-strain relationship, we exploit Hooke's law to derive Young moduli and Poisson ratios. Furthermore, to characterize the short-range order of amorphous structures, we calculate pair correlation functions as well as average coordination numbers [5]. To characterize long-range order properties, like the atomic transport properties, we compute the mean square displacements to obtain the self-diffusion coefficients [1]. Finally, we analyze shortest-path rings of the interconnection networks, which are related to the medium-range order. Here, we improved the algorithm of Franzblau by exploiting the sparsity of the distance matrix of the interconnection graph. This way, we obtain a computational complexity of the order $\mathcal{O}(Nn^{\frac{k}{2}} \log k)$ instead of $\mathcal{O}(N^2)$ to calculate all shortest-path rings of maximal length k of a given interconnection network, where n denotes the maximal coordination number [5].

3 Numerical Experiments, Results and Discussion

We have incorporated the computational methods described in section 2 into our existing MD software package TREMOLO, which is a load-balanced distributed memory parallel code [1]. All experiments were performed on our PC cluster Parnass2, which consists of 128 Intel Pentium II 400 MHz processors connected by a 1.28 GBit/s switched Myrinet. We first equilibrated the following periodic systems under normal pressure at 300 K, 600 K, 900 K, 1200 K and 1500 K; see also Fig. 1:

- Amorphous Si_3BN_5, $Si_3B_2N_6$, and $Si_3B_3N_7$ with 3831, 4070, and 4254 atoms.
- An about 44 Å long capped BN-NT with 456 atoms.
- *System I*: An about 36 Å long $(12, 0)$ continuous BN-NT with 360 atoms.
- *System II*: BN-NT of System I embedded in a $Si_3B_3N_7$ matrix with 4254 atoms.
- *System III*: Capped BN-NT embedded in a $Si_3B_3N_7$ matrix with 8508 atoms.
- *System IV*: Capped BN-NT embedded in a $Si_3B_3N_7$ matrix with 17016 atoms.

For the Si_3BN_5, $Si_3B_2N_6$, and $Si_3B_3N_7$ matrices, we computed pair correlation functions $g_{\alpha-\beta}$, average coordination numbers $n_{\alpha-\beta}$ and self-diffusion coefficients D_α, where $\alpha, \beta \in \{\mathrm{Si}, \mathrm{B}, \mathrm{N}\}$; see also Fig. 2. Here, we exploited the minima of $g_{\alpha-\beta}$ to determine the bonding distances and thus to calculate the average coordination numbers as well as to analyze shortest-path rings. Our results show that the self-diffusion coefficients, the average coordination numbers $n_{\mathrm{Si-Si}}$, $n_{\mathrm{B-N}}$ and $n_{\mathrm{N-B}}$ significantly increase and the average coordination numbers $n_{\mathrm{Si-N}}$ and $n_{\mathrm{N-Si}}$ significantly decrease for temperatures larger than 1200 K. Also witch respect to the tensile test, our computed stress-strain curves show that the Young moduli for a temperature of 1500 K is significant lower than for 1200 K; see Fig. 3. Furthermore, the results of the tensile test show that the fraction of the shortest-path rings with length $5 \leq k \leq 10$ decrease with an increase of the external stress. Finally, the stress-strain curves show that $Si_3B_3N_7$ has the highest Young moduli and the largest the elastic range compared to $Si_3B_2N_6$ and Si_3BN_5; see Fig. 3.

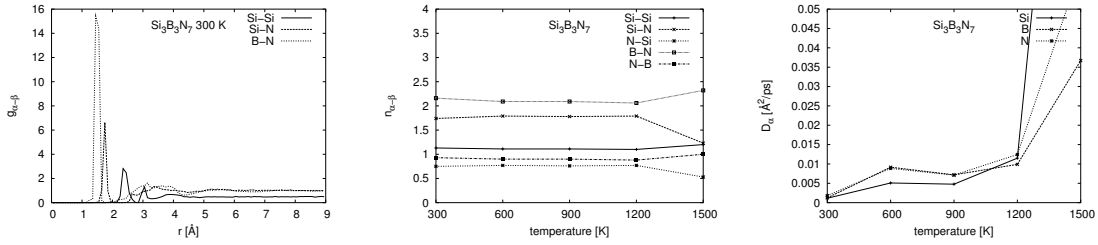

Figure 2: Partial radial distribution functions, average coordination numbers and self-diffusion coefficients for equilibrated $Si_3B_3N_7$.

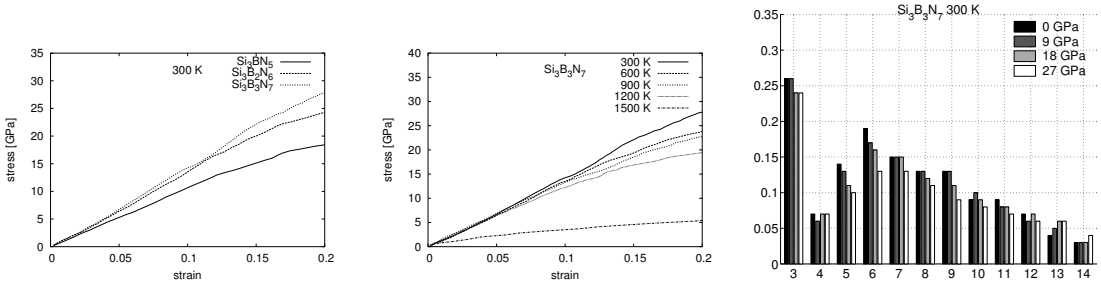

Figure 3: Stress-strain curves and distribution of shortest-ring paths for tensile tests.

For the composites System II, System III and System IV we performed tensile tests to compute the Young moduli and thus the reinforcement rates; see Tab. 1. Here, our results predict a reinforcement of about 12% in the case of System III and of about 6% in the case of System IV. For a nanocomposite, a macroscopic rule-of-mixtures (ROM) can be used to estimate its Young modulus depending on the volume fraction Ω_f of the nanofiber, the Young modulus E_f of the nanofiber and the Young modulus E_m of the matrix. This rule reads as

$$E_c = \Omega_f E_f + (1 - \Omega_f) E_m \,,$$

where E_c denotes the predicted Young modulus of the composite. For System II this estimation results in a relative error of 5% and less; see Tab. 2. For System IV we obtain values between 1.7% and 6.0% and for Sytem III we get values between 5.8% and 7.5% depending on the temperature. In the case of System III and System IV the relative error can be further reduced by using an extended ROM (EROM), which additionally takes the geometric distribution of the nanofiber into account:

$$E_c^{\text{ex}} = \left(\frac{1}{E_m} \frac{(L - L_c)}{L} + \frac{1}{E_c} \frac{L_c}{L} \frac{A}{A_c} \right)^{-1} .$$

Here, E_c^{ex} denotes the predicted Young modulus of the composite, L_c denotes the length of the nanofiber, L denotes the length of the system in direction of the longitudinal axis, R_{in} denotes the inner radius of the nanotube, A denotes the area of the transverse section and A_c is defined as $A_c = A - \pi R_{\text{in}}^2$; compare also Fig. 4.

Table 1: Calculated Young moduli E and Possion ratios ν.

	Tensile								
	$Si_3B_3N_7$		System I	System II		System III		System IV	
T [K]	E [GPa]	ν	E [GPa]	E [GPa]	ν	E [GPa]	ν	E [GPa]	ν
300	132.1	0.27	696.1	181.5	0.24	150.2	0.25	139.1	0.27
600	131.7	0.30	671.6	171.8	0.30	148.9	0.27	136.6	0.29
900	130.0	0.29	674.4	169.0	0.32	145.4	0.30	140.7	0.31
1200	129.5	0.32	657.8	164.2	0.30	145.1	0.32	140.1	0.36

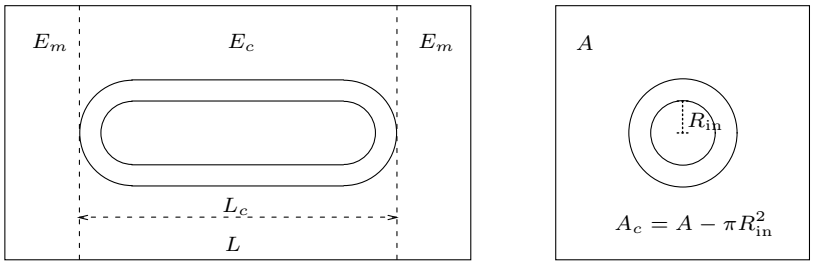

Figure 4: Schematic diagrams with respect to the EROM.

Table 2: The relative errors of the ROM and the EROM.

	System II	System III		System IV	
T [K]	ROM	ROM	EROM	ROM	EROM
300	-0.0284	0.0614	0.0356	0.0495	0.0279
600	0.0091	0.0580	0.0332	0.0598	0.0393
900	0.0143	0.0715	0.0456	0.0167	-0.0037
1200	0.0492	0.0749	0.0490	0.0198	-0.0012

4 Concluding Remarks

Our simulation results show that BN-NTs can be used to reinforce Si-B-N ceramics, at least theoretically. Now, experimental studies are needed to synthesize this suggested composite material also in practice and to determine its characteristic properties. More details related to our methods and results are given in [5].

5 Acknowledgments

This work was supported by a grant from the *Schwerpunktprogramm 1165* and the *Sonderforschungsbereich 611* of the *Deutsche Forschungsgemeinschaft*.

References

[1] M. Griebel, S. Knapek, G. Zumbusch, and A. Caglar. *Numerische Simulation in der Moleküldynamik. Numerik, Algorithmen, Parallelisierung, Anwendungen*. Springer, Berlin, Heidelberg, 2003.

[2] A. Caglar and M. Griebel. On the numerical simulation of fullerene nanotubes: $C_{100.000.000}$ and beyond! In R. Esser, P. Grassberger, J. Grotendorst, and M. Lewerenz, editors, *Molecular Dynamics on Parallel Computers, NIC, Jülich 8-10 February 1999*. World Scientific, 2000.

[3] M. Griebel and J. Hamaekers. Molecular dynamics simulations of the elastic moduli of polymer-carbon nanotube composites. *Computer Methods in Applied Mechanics and Engineering*, 193(17–20):1773–1788, 2004.

[4] M. Griebel and J. Hamaekers. Molecular dynamics simulations of polymer-carbon nanotube composites. In M. Rieth and W. Schommers, editors, *Handbook of Theoretical and Computational Nanotechnology*. American Scientific Publishers, 2005. In preparation.

[5] M. Griebel and J. Hamaekers. Molecular dynamics simulations of mechanical properties of boron-nitride nanotubes embedded in Si-B-N ceramics. SFB 611 preprint, University of Bonn, 2004.